

Chapter 9

Vapor Transport Model Verification

Having constructed a vapor transport model for the study of Directed Vapor Deposition, model verification studies were undertaken to assess the ability of the model to replicate different well characterized results presented in the literature. These studies examined the ability of Bird's two dimensional axisymmetric DSMC model to reproduce the carrier gas jet structure observed in Fig. 5.6. They also explored the ability of the BCT model to predict the distance between atomic collisions in a system for a given pressure (i.e. to estimate the mean free path correctly), the random walk motion of an individual argon atom in an argon gas volume at thermal equilibrium, and the energy loss for sputtered atoms traveling from sputtering target to deposition surface through various pressures of argon.

9.1 Verification of DSMC Results

To validate the flowfield results produced by the DSMC code, a simulation was run to reproduce the gas jet structure recorded in Fig. 5.6 a). To replicate this experimentally observed result, the DSMC code was configured to use argon as the carrier gas entering a chamber pressure of 50 Pa (0.375 Torr) with a nominal Mach number of 1.70 (mixing

chamber/process chamber pressure ratio = 5.40). The model's results are shown in comparison with the experimentally recorded flowfield structure (Fig. 9.1).

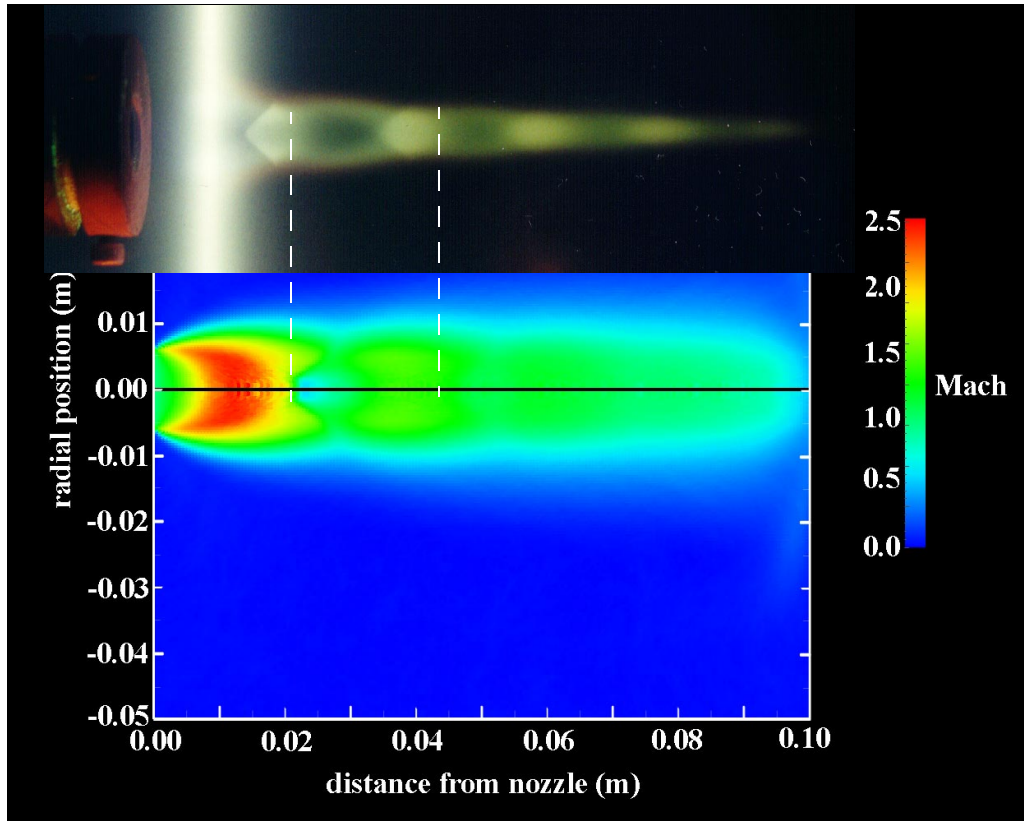


Figure 9.1 **Comparison of flowfield simulation with experimental result.** Comparison of DSMC output with experimental visualization demonstrates reasonable reproduction of actual flow structures. (Conditions: gas type = argon, chamber pressure = 50 Pa (0.375 Torr), pressure ratio = 5.40)

The comparison of model and experiment shows reasonable agreement between the two. Specifically, the location of the zone of silence, Mach disk, and secondary barrel shocks observed experimentally are replicated by the model. Note however that the model does not show the fast flow region narrowing as quickly as is observed experimentally. Conceivably, the ionization/excitation phenomenon which makes the flowfield visible experi-

mentally is not producing a profile of Mach number but rather of some other process variable like temperature or pressure. However, visualization of these two system variables with the DSMC code did not lead to a closer fit between experiment and model; the width of the core flow region remained essentially the same for all variables.

Another distinct result of the modeling is that, for the given pressure ratio, portions of the gas flow reach substantially higher Mach numbers than is suggested through the use of equation (2.4). This latter point probably highlights the limited validity of the one dimensional isentropic flow equations rather than a problem with the DSMC code.

An additional comparison between model and experiment was performed to replicate the flow structure of Fig. 5.6 d) for argon at a chamber pressure of 50 Pa and a pressure ratio of 16.7 (nominal $M = 2.5$). These results did not show the same level of agreement between model and experiment. The model predicted the Mach disk to be significantly further downstream than actually observed. This overprediction of the length of the zone of silence by the DSMC method has also been reported elsewhere by Boyd et al. [150]. In their study, Boyd et al. suggest that the discrepancy could be the result of selecting incorrect boundary or inlet conditions for the DSMC modeled regime. The discrepancy could also be the result of VHS and VSS approximations as discussed in section 2.2.5. Although the discrepancy is of concern, its effect upon the conditions simulated in Chapter 10 should be minimal since the simulated Mach numbers of 1.45, 1.75, and 1.95 are near the pressure ratio regime where good agreement has been demonstrated (Fig. 9.1).

9.2 BCT Model Verification

The validity of the BCT code was assessed through a set of model verification simulations. As highlighted in the flowchart of Fig. 8.5, model accuracy depends most impor-

tantly upon correct calculation of the vapor atom velocity vector following a collision event where assessment of the validity of the velocity vector involves verification of both its direction and magnitude. None of the BCT model verification tests described in this section relied upon the DSMC code. Rather than use a flowing gas field as an input, these verification studies employed just sixteen gridpoints to describe the temperature, pressure, and size of a cylindrical volume filled with argon gas at thermal equilibrium.

9.2.1. *Random walk*

Having demonstrated the ability of the BCT model to predict the distance between atomic collisions correctly, a study was undertaken to investigate whether or not the BCT model correctly computed the angle of deflection of the atoms involved in each collision event. For this purpose the model was configured to simulate the “random walk” of a thermalized argon atom in a volume of argon at equilibrium.

Random walk theory has been the subject of numerous books and articles and has been used throughout science to describe various processes such as surface diffusion of an atom (Fig. 9.2) and vapor phase diffusion in an equilibrium gas [225-227]. For the classic, pure

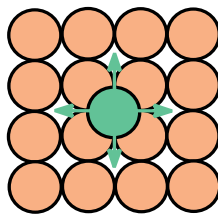


Figure 9.2 **Random walk on an atomic surface.** During surface diffusion, an atom on the surface of a crystal has an equal probability of jumping to any of the neighboring sites. This leads to random walk of the atom.

random walk problem of atomic surface diffusion on a perfect lattice, the atom illustrated

in Fig. 9.2 has an equal probability of jumping in any of four directions. Since it is equally probable that the atom will travel in any of the four directions for any jump, on average, there will be no net motion in any one direction. However, as time passes, the probability increases that the atom will be found some distance from its starting point. If a large number of atoms are simulated, after n jumps of a constant length l , the average straight line distance an atom has moved from its starting point will be $D = n\sqrt{l}$ [61]. (Note: This is not the total distance the atom has traveled, which would be $D = nl$.)

When applied to atomic diffusion in the vapor phase, random walk theory must account for subtle but important distinctions from the surface diffusion example. The most important difference is that vapor phase diffusion is not a pure random walk problem. In the surface diffusion example, the atom had an equal probability of jumping to any of the neighboring surface sites. In the vapor transport problem, such an equal probability would mean that, following a collision event, the atom being tracked has an equal probability of leaving a collision point in any direction. This is not the case for vapor phase diffusion because the velocity of the tracked atom coming into the collision event biases its future direction of travel. Chapman and Cowling summarize the effect of this bias [143]:

After a collision with another molecule the velocity of a given molecule will, on the average, still retain a component in the direction of its original motion. This phenomenon is known as the persistence of velocities after collision. As a consequence, the average distance traversed by a molecule in the direction of its velocity at a given instant, before (on the average) it loses its component motion in that direction, is somewhat greater than its (Tait) mean free path.

Fig. 9.3 illustrates a single “jump” for the case of vapor phase diffusion. Surprisingly, an analytical solution describing the magnitude of this forward bias does not appear in the literature to date [228]. Thus, simulation of vapor phase random walk will provide only a

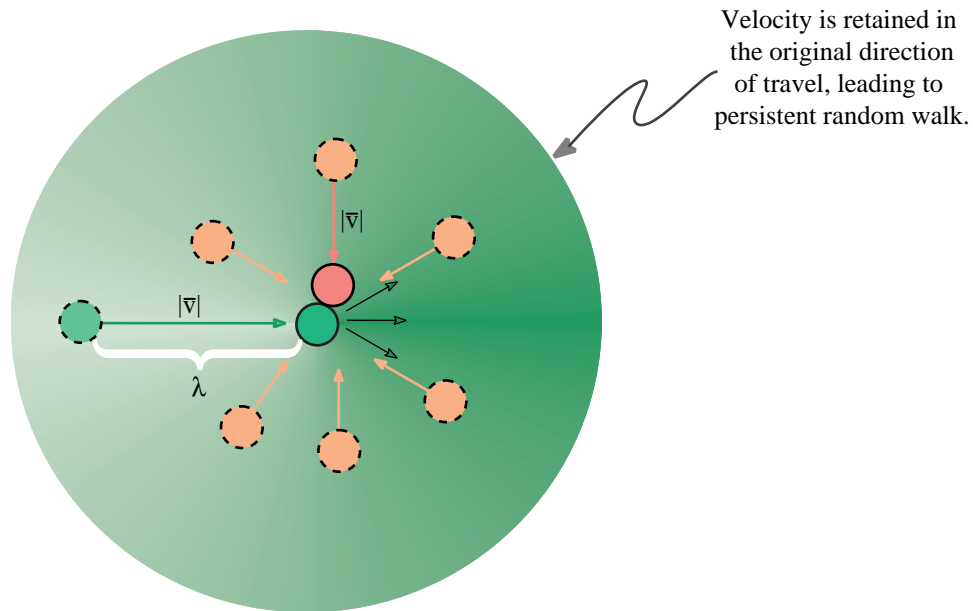


Figure 9.3 **Persistent random walk during vapor phase diffusion.** Persistence of the velocity of the atom being tracked results in a probability density function for the angle of scattering which is not uniform over all angles but rather a function of the velocity of the atom being tracked. A forward bias exists even though the atom with which it collides has an equal probability of entering the collision from any direction and on average has the same velocity magnitude as the tracked atom.

general measure of the BCT code's validity. Rather than describing the distance traveled by $D = n\sqrt{l}$, it should be possible to describe the distance by $D = n\sqrt{\lambda_e}$ where the effective mean free path λ_e is slightly greater than the actual, measured value of λ (as Chapman and Cowling have explained). Thus a plot of distance from the starting point versus number of collision events should show that $D = n\sqrt{\lambda}$ slightly underpredicts the distance traveled by a consistently small amount ($\sqrt{\lambda_e/\lambda}$).

It should also be noted that random walk theories of vapor phase transport employ hard spheres with no interatomic potentials active between them. (The model is capable of sim-

ulating random walk in a system employing interatomic potentials and could be used as a tool for developing a simple random walk expression in this system similar to $D = n\sqrt{\lambda}$.) Fig. 9.4 shows the results of a hard sphere simulation of vapor phase random walk in which no interatomic potential is active. The figure compares this prediction with than of pure random walk as described $D = n\sqrt{\lambda}$.

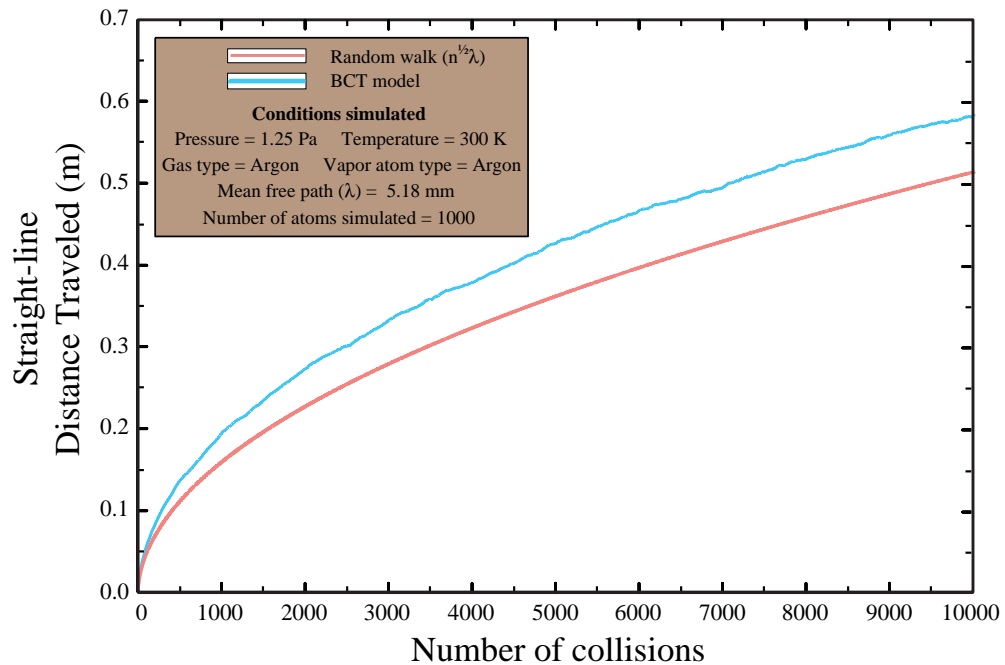


Figure 9.4 **Pure vs. persistent random walk.** The BCT simulation of random walk for an argon atom in thermal equilibrium with a chamber full of argon shows the expected forward bias which makes the atom travel slightly further than predicted by pure random walk theory.

The results plotted in Fig. 9.4 represent the average distance traveled by 1000 argon atoms from their starting point as a result of 1 to 10,000 collisions with background argon atoms (i.e., the straight-line distance from start point to finish point). Each of the 1000 atoms was tracked individually with the average distance traveled per mean free path step computed after all atoms had been simulated. The average mean free path for all diffusion during the

simulation was 5.18 mm, and this value of λ was used to compute the pure random walk line shown in Fig. 9.4. The “distance traveled” results generated by the BCT model predict that the vapor atom will travel 11.5 - 13.5% further each mean free path step than predicted by pure random walk theory (i.e. $\lambda_e/\lambda = 1.115 - 1.135$). While there is no vapor phase random walk theory against which to compare this result, the bias generated by the BCT model is consistent over all 10,000 steps, and it represents a bias in the direction predicted by Chapman and Cowling. Thus, it appears that the model reasonably predicts the direction of the vapor atom after a collision.

9.2.2. Atomic energy loss

To investigate whether or not the BCT model correctly transfers energy between two colliding atoms, the model was configured to simulate a sputtering system in which high energy copper atoms departing a sputtering target travel through an argon gas atmosphere. During their traverse of the sputtering chamber, the energetic copper atoms collide with argon gas atoms (in thermal equilibrium at 350K), leading to a reduction in copper atom kinetic energy. Sputtered atom energy was measured at fixed distances from the target (2.50 and 5.00 cm) for different chamber pressures (10^{-6} - 100 Pa) to reveal the dependence of kinetic energy loss upon chamber pressure. To assess the validity of the BCT model’s results, the energy loss results produced by the model were compared with the models of others [229, 230] and with one of the few sets of experimental data available in the literature for sputtered atom energy loss versus argon chamber pressure and distance [231].

The initial copper atom kinetic energy distribution leaving a sputtering target is substantially different than that of atoms leaving an e-beam evaporant source [60]. A sputtered atom energy distribution based upon study of the literature [232] was incorporated into the

BCT model to facilitate more accurate simulation of sputtering (Fig. 9.5). Interatomic

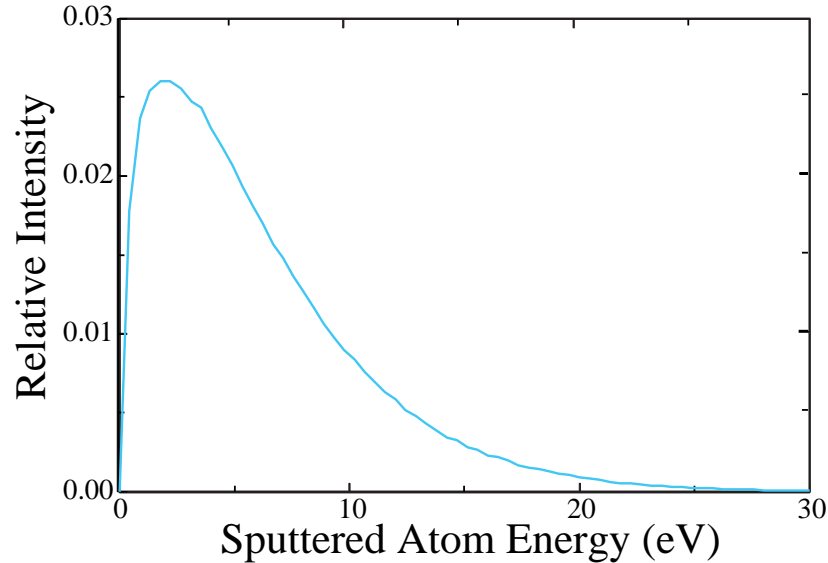


Figure 9.5 **Energy distribution of atoms leaving a sputtering target.** While most atoms leaving the target have energies less than 10 eV, a number of atoms have energies well above this level, creating a high energy tail on the energy distribution.

potentials were employed for these simulations with $\chi_{\text{cutoff}} = 0.01$ radians. To allow comparison with the results reported in the literature, the average energy of the sputtered atoms as they left the sputtering target was 5.1 eV.¹ Atoms were allowed to leave from a target 5.08 cm in diameter which was centered above the round 10.00 cm diameter substrate surface. During calculation of the momentum transfer during a collision event, equation (8.17), used to distribute gas atom velocities in the flowing carrier jet, was replaced with the more common Maxwell-Boltzmann distribution (equation (8.18)) used to describe atom velocities in a thermal equilibrium gas [223].

¹ The authors of the experimental data suggest that the average starting energy of their copper atoms was much higher, ~13 eV. This seems unreasonable given the reported accelerating voltage of their system, 410 V [231], and the sputtered atom energy distribution generated by other similar sputtering systems [232].

The results of these simulations are plotted in Figs. 9.6 and 9.7 while the actual numerical results are recorded in Tables 9.1 and 9.2. Note that for each set of conditions investi-

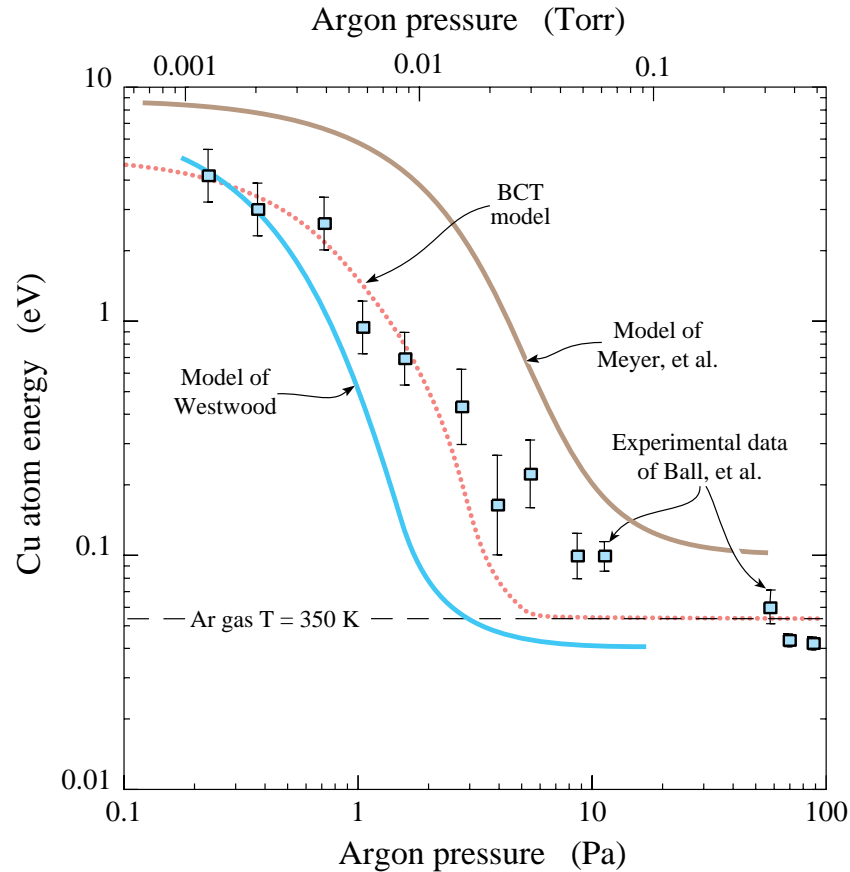


Figure 9.6 **Energy loss at 2.5 cm.** The results of the BCT model for a target to substrate distance of 2.5 cm show better agreement with experimental results than the modeling efforts of Westwood [229] or Meyer, et al. [230].

gated, a minimum of 10,000 atoms had to reach the measurement distance to create a valid simulation. Study of various data set sizes between 100 and 20,000 atoms indicated that results averaged from 10,000 atoms reaching the 10.0 cm diameter substrate represented well converged solutions. While the results in Figs. 9.6 and 9.7 do not exactly reproduce the experimental data of Ball, et al. [231], they do represent a closer fit to the experimental data than previous modeling efforts by Westwood [229] and Meyer, et al. [230].

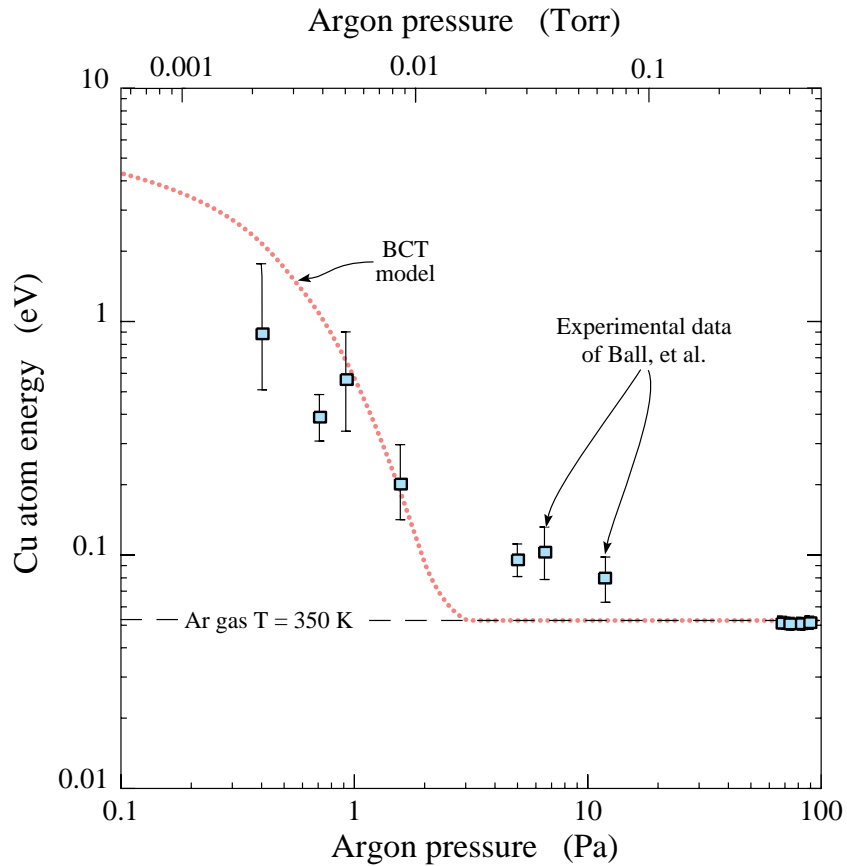


Figure 9.7 **Energy loss at 5.0 cm.** When compared to the experimental data of Ball, et al. [231], the BCT model underpredicts sputtered atom energy loss at low chamber pressures and overpredicts it at higher pressures for a target to substrate distance of 5.0 cm.

The fit of the BCT data to the experimental results becomes more encouraging when the findings of Ball, et al. are examined more closely. Ball et al. suggest that, at low argon chamber pressures, their experimental method underestimates the actual energy of the sputtered atoms in part because of their assumption that the sputtered copper atoms have a Maxwell-Boltzmann energy distribution just after leaving the sputtering target [231]. Given this acknowledged error, the energy predictions of the BCT model could be quite close to the actual sputtered atom energies for chamber pressures below a few Pascals.

Table 9.1: Copper atom energy 2.5 cm from target

Chamber Pressure (Pa)	Atoms Simulated	Deposition Efficiency (%)	Average Energy (eV)
10^{-6}	11,000	93.87	5.128
0.1	11,000	92.05	4.690
0.2	12,000	89.52	4.273
0.5	13,000	80.94	3.033
1.0	15,000	68.81	1.600
2.0	21,000	47.88	0.505
3.0	29,000	35.48	0.149
5.0	43,000	23.32	0.058
7.0	59,000	17.03	0.052
10.0	84,000	12.03	0.053

Table 9.2: Copper atom energy 5.0 cm from target

Chamber Pressure (Pa)	Atoms Simulated	Deposition Efficiency (%)	Average Energy (eV)
10^{-6}	14,000	71.95	5.078
0.1	15,000	67.91	4.346
0.2	16,000	63.30	3.534
0.5	20,000	50.01	1.891
1.0	29,000	35.48	0.609
2.0	49,000	20.70	0.094
3.0	70,000	14.43	0.053
5.0	112,000	8.95	0.052

At higher chamber pressures the BCT model predicts complete vapor atom thermalization before it is observed experimentally. The exact cause of this discrepancy is unclear but could result from the presence of argon ions in the actual sputtering system with smaller scattering cross-sections, from the sputtered atoms in the experimental setup having a different initial energy distribution than that used (e.g. a longer, more significant high energy

tail), or from the use of an interatomic potential in the BCT model which incorrectly predicts the dependence of scattering angle (and thus energy loss) upon interatomic separation. For some portion of the distance between sputter target and deposition substrate, argon ions in the actual sputtering system would be under the influence of the electric field which accelerates them into the target to generate copper atoms for film creation. As a result, their velocities cannot be described by the thermal equilibrium Maxwell-Boltzmann distribution, taken at 350 K. Instead, their higher velocities decrease their cross-section, increase the distance between collisions with copper atoms, and lead to a persistence of copper atom energy at higher chamber pressure. Despite these discrepancies, the BCT results presented in Figs. 9.6 and 9.7 suggest that the model predicts energy transfer during collisions with reasonable accuracy given the limitations of the equations upon which it is based.

Finally it should be noted that the experimental data reported by Ball et al. does not completely agree with their assertion that the argon gas temperature in their chamber was 350 K. Serway et al. [223] note that, given a Maxwell-Boltzmann argon velocity distribution, the average velocity of atoms in the system is given by:

$$v_{avg} = \sqrt{\frac{8kT}{\pi m}} \quad (9.1)$$

Calculations based on this equation show that for argon atoms at 350 K, copper atoms will have approximately 0.061 eV of energy once they have been completely thermalized. This energy level is represented as a dashed line in Figs. 9.6 and 9.7. This energy level is above the energy level reported for certain experimental measurements. To place the line below the lowest experimental data would suggest that the gas temperature in the chamber was as low as 230 K. This seems too cold, suggesting that either the Maxwell-Boltzmann dis-

tribution does not exactly predict the velocity distribution of the argon or that the experimental data results are not completely correct.

9.3 Summary

The results of this chapter show reasonable agreement between independent experiments and DSMC/BCT vapor transport model results, and they demonstrate an ability of the model to replicate expected trends. Thus, with some degree of confidence the model can now be applied to a study of Directed Vapor Deposition deposition results reported in Chapter 7. The goal of Chapter 10 is to use the vapor transport model to provide additional insight into Directed Vapor Deposition's low vacuum material synthesis behavior.